JACS
JOURNAL OF THE AMERICAN CHEMICAL SOCIETY
Article
pubs.acs.org/JACS

The Importance of Hydrogen Bonding to Stereoselectivity and Catalyst Turnover in Gold-Catalyzed Cyclization of Monoallylic Diols

Thomas Ghebreghiorgis,[†] Berenger Biannic,[†] Brian H. Kirk,[‡] Daniel H. Ess,*[,‡] and Aaron Aponick*[,†]

[†]Department of Chemistry, University of Florida, Gainesville, Florida 32611, United States
[‡]Department of Chemistry and Biochemistry, Brigham Young University, Provo, Utah 84602, United States

Supporting Information

ABSTRACT: Density functional calculations and experiment were used to examine the mechanism, reactivity, and origin of chirality transfer in monophosphine Au-catalyzed monoallylic diol cyclization reactions. The lowest energy pathway for cyclization involves a two-step sequence that begins with intramolecular C−O bond formation by *anti*-addition of the non-allylic hydroxyl group to the Au-coordinated alkene followed by concerted hydrogen transfer/*anti*-elimination to liberate water. Concerted S_N2'-type transition states were found to be significantly higher in energy. The two-step cyclization pathway is extremely facile due to hydrogen bonding between diol groups that induces nucleophilic attack on the alkene and then proton transfer between diol groups after C−O bond formation. Importantly, intramolecular proton transfer and elimination provides an extremely efficient avenue for catalyst regeneration from the Au−C σ-bond intermediate, in contrast to other Au-catalyzed cyclization reactions where this intermediate severely restricts catalyst turnover. The origin of chirality transfer and the ensuing alkene stereochemistry is also the result of strong hydrogen-bonding interactions between diol groups. In the C−O bond-forming step, requisite hydrogen bonding biases the tethered nucleophilic moiety to adopt a chair-like conformation with substituents in either axial or equatorial positions, dictating the stereochemical outcome of the reaction. Since this hydrogen bonding is maintained throughout the course of the reaction, establishment of the resultant olefin geometry is also attributed to this templating effect. These computational conclusions are supported by experimental evidence employing bicyclic systems to probe the facial selectivity.

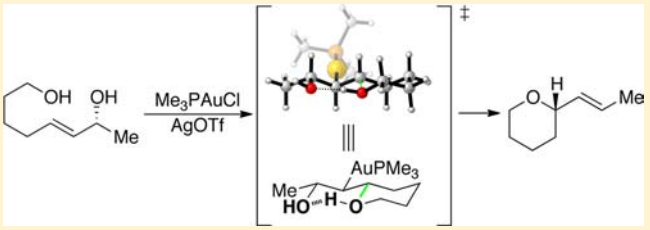

INTRODUCTION

The use of gold complexes to catalyze organic transformations has become an extremely active area of research, owing to the ease of handling the catalysts, their functional group compatibility, and the broad array of reactions that can be effected under relatively mild conditions.[1] Among the variety of Au-catalyzed reactions developed, the addition of heteroatom nucleophiles to carbon−carbon π-bonds (alkynes, alkenes, allenes) stands as one of the most powerful transformations and has therefore been the subject of continuous development. In 1998, Teles and co-workers reported the addition of alcohol nucleophiles to alkynes catalyzed by Ph_3PAu^+.[2] Since then, a large number of other groups have expanded the scope of the reaction to include additional heteroatom nucleophiles and also allene and alkene π-bonds.[1,3] The progression of this work has been reviewed.[1,3] However, many details about these transformations, such as the identity of the active catalyst (Au complex or protic acid), remain unresolved.[4]

In the reactions of heteroatom nucleophiles with olefins, one detail that is not fully understood is why the reaction conditions required are typically much harsher than the conditions required for allenes and alkynes (Scheme 1).[5] In these reactions, studies to probe the identity of the active catalyst and relevant catalytic intermediates have turned up a variety of interesting results. One such mechanistic detail is that

Scheme 1. Reaction Conditions for Au-Catalyzed Hydroalkoxylation Reactions

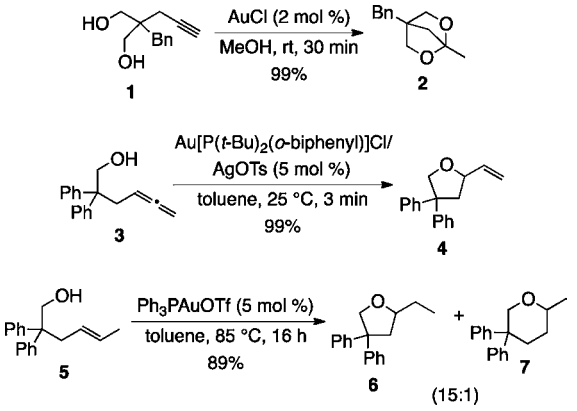

protonation of Au−C_{sp^3} σ-bond intermediates is difficult,[6] presumably much more so than that of Au−C_{sp^2} σ-bond intermediates, and therefore protodeauration of intermediate σ-Au complexes in reactions of olefins is challenging and is likely the origin of slow turnover frequencies. Direct experimental

Received: June 28, 2012
Published: September 4, 2012

dx.doi.org/10.1021/ja306333a | J. Am. Chem. Soc. 2012, 134, 16307−16318

evidence involving the protonation step was reported on the presumed hydroamination intermediate **8** (Scheme 2), isolated after *anti*-aminoauration in the presence of base.[7] Treatment of this σ-complex with TsOH for 1 h in $CDCl_3$ resulted in a 60:40 mixture of **10**:**8** with no protodeauration product **9** observed. Calculations on this system are in agreement with the experimental evidence and indicate that the elimination pathway (**8**→**10**) is lower in energy than the protodeauration pathway (**8**→**9**).[7]

Scheme 2. Studies on the Protonation of σ-Au Complexes

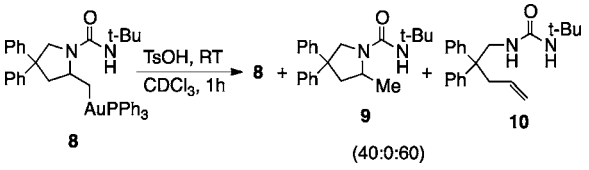

Recently, there has been significant interest in harnessing σ-Au intermediates for alternative uses, and, as competing reactions that are often problematic with M−C_{sp^3} organometallics such as protodemetalation are reduced, the ability to do so with Au−C_{sp^3} σ-complexes may offer practical advantages.[8] Reported examples of further functionalization of Au−C_{sp^3} σ-bonds include cross-coupling reactions, oxidative coupling, reactions with other nucleophiles, halogenation, and oxidation reactions.[8,9] Several examples shown in Scheme 3 illustrate efficient addition of X−R to Au−C bonds.[9]

Scheme 3. Functionalization Reactions of σ-Au Complexes

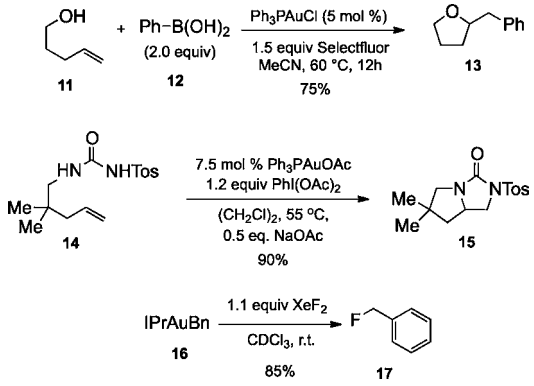

One of our groups has also developed Au-catalyzed reactions that proceed without protodeauration of the σ-Au intermediate. In 2008, Aponick and co-workers reported the Au-catalyzed addition of alcohols to the π-bond of allylic alcohols (Scheme 4),[10] which allows these simple electrophiles to function as allene surrogates in Au-catalyzed reactions.[5b,11] These systems consist of a nucleophilic alcohol tethered to an allylic alcohol such as **18**. By the action of a gold(I) catalyst, these diols cyclize to form 2-vinylheterocycles **19** instead of forming the hydroalkoxylation product **20** resulting from protodeauration. This reaction is quite general, and, in addition to alcohols, heteroaromatic and nitrogen nucleophiles have since been reported as well as substrates with propargylic alcohols as electrophiles.[12,13]

Scheme 4. Au-Catalyzed Addition/Elimination Reactions

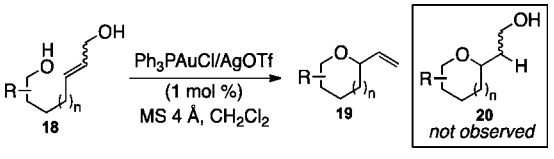

The observation of an elimination reaction was somewhat unexpected because the hydroxyl group is a poor leaving group and the reactions are typically rapid, reaching completion in less than 1 h. Additionally, in contrast to the reaction conditions required for intramolecular hydroalkoxylation of isolated olefins (5 mol % catalyst, toluene, 85 °C, 16 h),[14] these conditions are extremely mild (standard conditions: 1 mol % catalyst, CH_2Cl_2, room temperature, 1 h), and the reactions even proceed at −78 °C, albeit slowly.[15] From the outset, we were intrigued by the reaction mechanism and considered possible explanations for this disparate reactivity and also the high selectivity observed (initially diastereoselectivity and later enantioselectivity, *vide infra*). The transformation constitutes a formal S_N2' reaction, and, of the conceivable pathways, we thought the most plausible would likely be either a cationic mechanism that could possibly involve the formation of a π-allylgold complex[16] (pathway I, Scheme 5), a concerted S_N2' pathway (pathway II),

Scheme 5. Possible Reaction Pathways

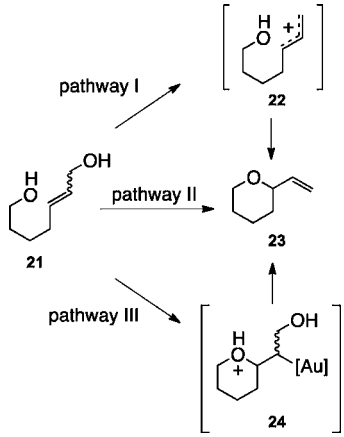

or a stepwise addition/elimination sequence (pathway III). We have now undertaken a combined experimental−computational interplay to distinguish among these pathways and clarify possible alternatives that have been proposed.[10,17,18] Herein we report results that reveal the importance of hydrogen bonding in substrate design that allows for efficient catalytic turnover of σ-Au intermediates from allylic alcohol substrates. In addition, our mechanistic analysis also explains the very high levels of stereoselectivity observed in these dehydrative cyclization reactions.

■ COMPUTATIONAL DETAILS

All stationary points were confirmed as minima or transition structures by normal-mode vibrational analysis in Gaussian 09.[19] The M06 density functional was used due to its superior performance for organometallic systems.[20] For the Au metal center the LANL2DZ pseudopotential basis set was used in conjunction with the 6-31G(d,p) basis used for all other atoms. All optimizations included implicit dichloromethane solvent effects using the SMD solvent model.[21] Solution-phase 298 K free energies (Δ*G*) were estimated by correction of standard-state gas-phase free energies with SMD solvation free energies (ΔG_{solv}). Reported 298 K enthalpies include ΔG_{solv}

dx.doi.org/10.1021/ja306333a | J. Am. Chem. Soc. 2012, 134, 16307−16318

correction. All energies are reported in kcal/mol. All bond lengths are reported in Å.

RESULTS AND DISCUSSION

In 2008, Aponick and co-workers reported the reaction illustrated in Scheme 4.[10] Surprisingly, exposure of both *cis*- and *trans*-olefins **25** and **26** to the reaction conditions resulted in the formation of the cyclized product **27**, containing a *trans*-double bond in comparable yield and after the same reaction time (Scheme 6). This result was intriguing to us and suggested several possible reaction mechanisms.

Scheme 6. Reactions of *cis*- and *trans*-Olefins

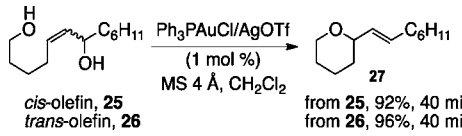

Although Au(I) complexes are widely considered soft π-acids, they also can act as more traditional Lewis acids,[22] and these data seemed to initially suggest that a cationic or metal-bound cation (π-allylgold) species may be an intermediate. While an intermediate cation may lead to a mixture of products, in our laboratory only *trans*-olefin products have been observed to date. In contrast, Widenhoefer has reported the isolation of *cis*-olefin products with amine nucleophiles,[12g] and, as will be discussed below, Robertson reported forming *cis*-2-alkenyltetrahydrofurans in a synthesis of (+)-isoaltholactone.[18] To test this notion, the olefins **28** and **29** were prepared and treated under the reaction conditions. If the mechanism was cationic in nature, both substrates would be predicted to undergo ionization, forming a cation or the corresponding π-allylgold complex, and after cyclization, both form 2-vinyltetrahydropyran **23** (Scheme 7). In the event, the standard substrate **28**

Scheme 7. Comparison of Standard and Alternative Allylic Alcohol Substrates

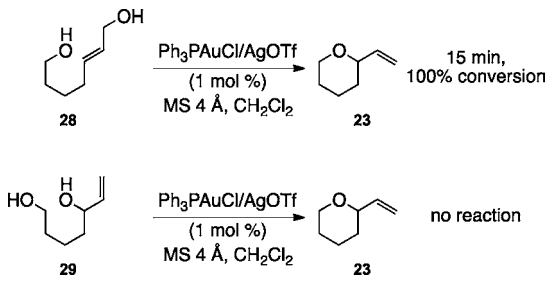

did indeed cyclize, consuming the starting material to form **23** in 15 min. In contrast, no reaction was observed with **29**, even under more forcing conditions such as increased catalyst loading, heating to reflux in dichloroethane, or using $AuCl_3$ as catalyst.[10]

These experiments seem to rule out the likelihood of forming a discrete allylic carbocation along the reaction pathway. This is further supported by density functional theory (DFT) calculations, which show that possible cationic intermediates can be ruled out. Although gold hydroxide complexes are known,[23] Scheme 8 shows that the computed Au-mediated heterolytic bond dissociation to give allyl cation **31** and $HOAu(PMe_3)$ **32** requires an enthalpy change (ΔH) of 42.7 kcal/mol and a free energy change (ΔG) of 27.0 kcal/mol

Scheme 8. Reaction Enthalpies for Possible Carbocation Pathways[a]

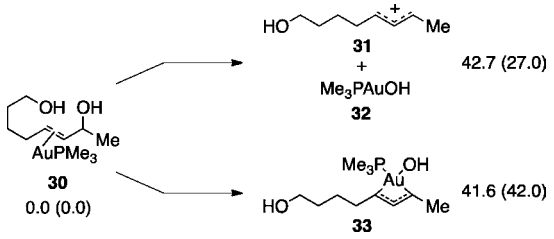

[a]Free energies are given in parentheses (kcal/mol).

relative to cationic $Au(PMe_3)$ coordinated diol **30**. Similarly high in energy, insertion of cationic $(PMe_3)Au^+$ into the carbon oxygen bond of the hydroxyl group to give **33** requires ΔH and ΔG values of 41.6 and 42.0 kcal/mol, respectively.

Based upon these results, an alternative explanation for forming the *trans*-olefin **27** from both **25** and **26** was required. This led to the examination of enantioenriched substrates containing a chiral center at the carbon bearing the allylic hydroxyl group.[24] It was found that substrates differing in olefin geometry but with the same absolute stereochemistry at the allylic alcohol carbon produced enantiomeric products with only a small amount of enantiomeric excess (ee) lost during the reaction (Scheme 9). The stereochemical transfer also

Scheme 9. Chirality Transfer

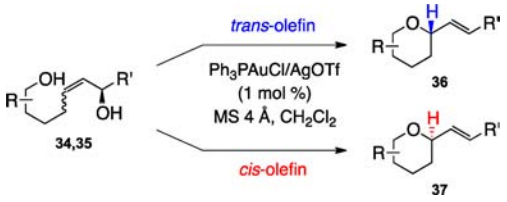

functioned in the same fashion when additional stereocenters were present in the acyclic starting materials to selectively yield diastereomeric products differing in the absolute stereochemistry at the newly formed stereocenter.[24] This allows for selective access to either enantiomer of product from a single chiral propargyl alcohol by reduction of the alkyne to either a *cis*- or *trans*-alkene followed by Au-catalyzed dehydrative cyclization.

Interestingly, the sense of chirality transfer in the products was entirely consistent, leading to the facile prediction of the absolute stereochemical outcome of the reaction (Figure 1). This led to the proposal of the catalytic cycle shown in Scheme 10, which allowed for the possibility of either a *syn*- or *anti*-alkoxyauration addition mechanism followed by elimination of water to form the resultant olefin.

It should be noted that the stereochemistry observed in the overall transformation is consistent with a concerted *syn*-S_N2' reaction, which could not be ruled on the basis of any experimental data. In fact, Roberston and co-workers observed the reactions in Scheme 11 and presented a mnemonic that is highly suggestive of a concerted *syn*-S_N2' mechanism (Figure 2).[18] It should be noted that the ancillary ligand (Ph_3P) is not included but would still be present and coordinated to the metal center.

A large amount of work on the mechanism of S_N2' reactions has been done, and both concerted and stepwise *syn*- and *anti*-

dx.doi.org/10.1021/ja306333a | J. Am. Chem. Soc. 2012, 134, 16307−16318

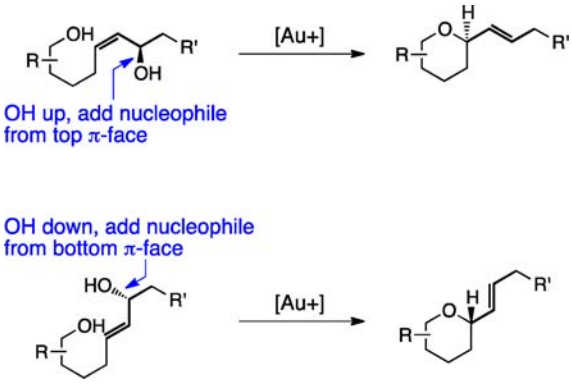

Figure 1. Predictive model.

Scheme 10. Aponick's Proposed Catalytic Cycle

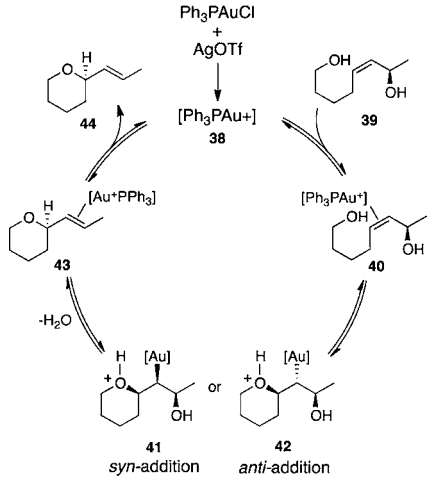

S_N2' mechanisms are known,[25] but there have been no reports on the mechanism of Au-catalyzed direct S_N2' reactions of allylic alcohols. On the theoretical forefront, Streitweiser has recently revisited the S_N2' reaction of allylic halides and has outlined several interesting aspects of the reaction mechanism with regard to coordination and solvation.[26] If these data are adapted to the present system, a *syn*-S_N2' mechanism would be predicted if the catalyst could coordinate to both the incoming hydroxyl group nucleophile and departing −OH leaving group in a manner similar to the way Robertson's mnemonic has presented the catalyst/substrate interaction (Figure 2). As mentioned above, Au(I) complexes can in fact serve as oxophilic Lewis acids;[22] however, this is not the role that has traditionally been proposed in gold catalysis.[1] Furthermore, while three-coordinate gold(I) complexes are known,[27] this is not the typical role proposed for the catalyst in Au-catalyzed reactions,[1] and in fact an increasing number of crystal structures showing two-coordinate, linear Au(I) π-complexes have been reported.[28]

Robertson also notes in his report that the structural elements of the substrate may play a role in determining the stereochemical outcome of the reaction.[18] The observation of *cis*-olefin products and truncated fidelity in the chirality transfer may be attributed to the presence of other stereocenters. Furthermore, the 2,5-*cis*/*trans* relative stereochemistry is also affected by these additional stereocenters, providing mostly 2,5-*trans* products, in contrast to the preference for 2,5-*cis* observed in systems without non-stereogenic allylic alcohols.[10] Aponick

Scheme 11. Robertson's THF Synthesis

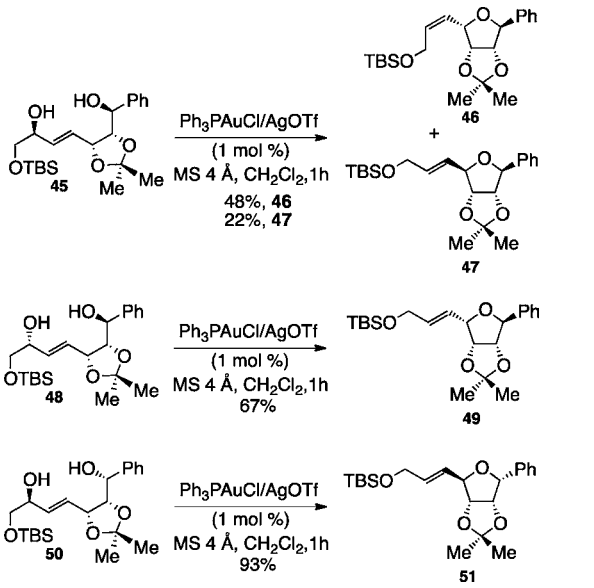

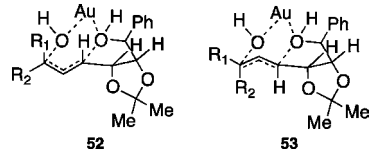

Figure 2. Robertson's mnemonic.

and co-workers also proposed that a secondary structural element, namely hydrogen bonding, may perform an important function in transition-state assembly.[24,29] Gathering further experimental evidence for the mechanism was challenging, and we have now turned to DFT to decipher between concerted and stepwise formal S_N2' pathways as well as to probe the importance of hydrogen bonding and the factors dictating the transfer of chirality.

To begin, we explored several possible mechanisms for (trimethylphosphine)gold-catalyzed cyclization of the model allylic diol **54** (Scheme 12). Cyclization of diol **54** leads to only one of four possible tetrahydropyran diastereomers (**55**) shown in Scheme 12.

As described above, the formation of an allyl cation followed by cyclization required the cleavage of the C−O bond in a highly endergonic process and was discounted for this reason. We have considered several other possible mechanisms for the cyclization of diol **54** (Scheme 13). The second mechanism considered is also a stepwise process leading formally to the

Scheme 12. Allylic Diol Cyclization Studied with Density Functional Calculations

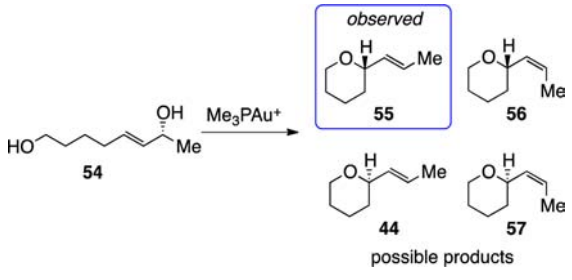

dx.doi.org/10.1021/ja306333a | J. Am. Chem. Soc. 2012, 134, 16307−16318

Scheme 13. Possible Cyclization Pathways

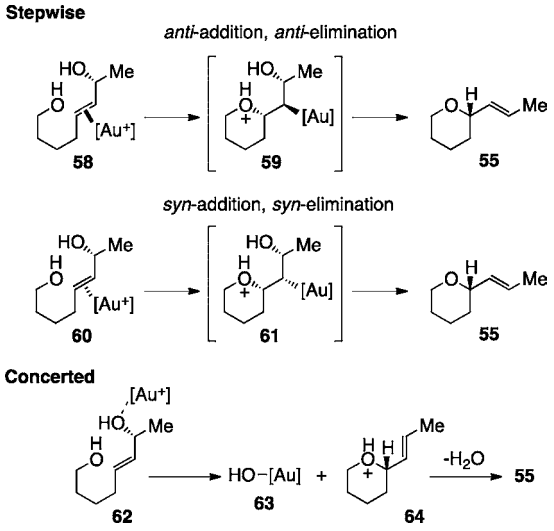

formation of S_N2' products. There are two possibilities that lead to the observed stereochemistry in the chirality transfer experiments. These possible mechanisms differ in the stereochemistry of the addition and elimination. The first step of the mechanism would involve a *syn*- or *anti*-addition of the hydroxyl group and gold catalyst to the alkene, with the second step of these pathways requiring the corresponding *syn*- or *anti*-β-hydroxide elimination. Lastly, we also considered direct, concerted S_N2' pathways.

Stepwise S_N2' addition begins with intramolecular addition of the non-allylic hydroxyl group to the alkene. This can occur with the gold catalyst coordinated to the same or opposite face of the alkene as the allylic hydroxyl group and results in net *syn*- or *anti*-alkoxyauration. Scheme 14 shows the lowest energy

Scheme 14. Lowest Energy Stepwise *anti*-Addition, *syn*-Addition, and Concerted S_N2' Transition States

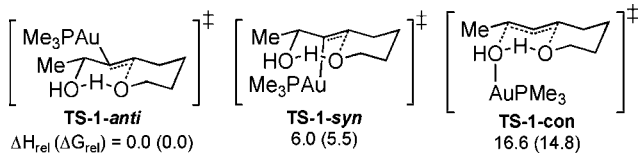

transition states for *syn*- and *anti*-alkoxyauration. The overall lowest energy transition state, **TS-1-*anti***, involves the cationic Me_3PAu^+ coordinating *anti* to the forming C−O bond. Pathways involving similar low-energy *anti*-addition transition states have also previously been proposed on the basis of DFT calculations.[30] The alternative *syn*-addition transition state, **TS-1-*syn***, is 6.0 kcal/mol higher in enthalpy relative to **TS-1-*anti*** and 5.5 kcal/mol higher in free energy relative to **TS-1-*anti***. As will be discussed in detail later, in both **TS-1-*anti*** and **TS-1-*syn*** the diol groups participate in intramolecular hydrogen bonding. Without diol hydrogen bonding, *anti*- and *syn*-addition transition states are ∼5−15 kcal/mol higher in energy.

Besides these stepwise *anti*- and *syn*-addition transition states, there is also the possibility for a concerted *syn*-S_N2' mechanism (Scheme 13). Scheme 14 depicts the concerted transition state, **TS-1-con**, where the cationic Me_3PAu^+ coordinates the allylic hydroxyl group to assist in C−O bond cleavage. In this transition state, similar to **TS-1-*anti*** and **TS-1-*syn***, there is hydrogen bonding between diol groups, but **TS-1-con** is 16.6 kcal/mol higher in enthalpy and 14.8 kcal/mol higher in free energy relative to **TS-1-*anti***. We were unable to locate transition states where the cationic Me_3PAu^+ served to template the reaction by coordination to both hydroxyl groups of the diol (i.e., **52**/**53**, Figure 2). One likely reason why **TS-1-con** is much higher in energy than **TS-1-*anti*** is that coordination of cationic Me_3PAu^+ to the allylic hydroxyl group greatly diminishes the ability of the oxygen to act as an electron pair donor in the hydrogen-bonding interaction.

The activation enthalpy for **TS-1-*anti*** ($\Delta H^{\ddagger}$) is 8.4 kcal/mol, and the free energy of activation ($\Delta G^{\ddagger}$) is 11.5 kcal/mol relative to the alkene−Au(PMe_3) complex **58** (Scheme 13, Figure 3). In **TS-1-*anti***, the forming C−O has a partial bond

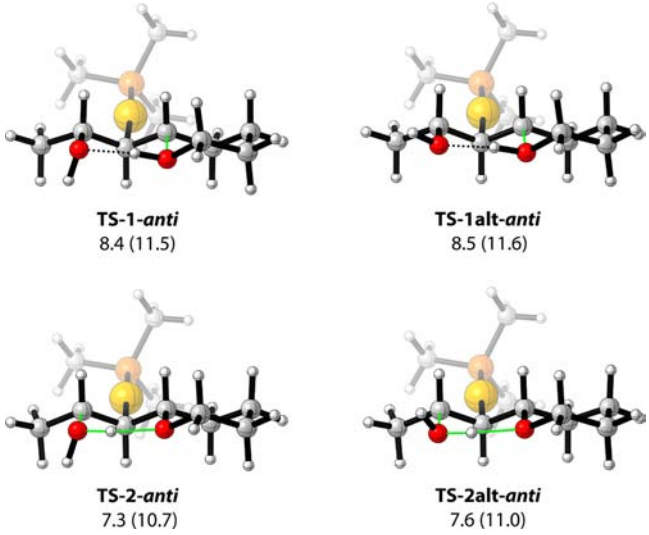

Figure 3. Two lowest energy alkoxyauration alkene addition and water release transition states. Enthalpies (free energies) are reported relative to gold diol complex (*E*)-**58** (kcal/mol).

length of 1.84 Å, and the π-bond is stretched from 1.37 Å in (*E*)-**58** to 1.44 Å in **TS-1-*anti***. The hydrogen-bonding interaction in this transition state is ideal, with a distance of 1.72 Å between the allyl hydroxyl group oxygen atom and the non-allylic hydroxyl group proton. In Figure 3, the three-dimensional representation of **TS-1-*anti*** shows that the hydrogen-bonding interaction occurs in a nearly collinear arrangement. The allylic hydroxyl group can be oriented in two different conformations that give rise to nearly energetically equivalent transition states **TS-1-*anti*** and **TS-1alt-*anti***.

The complete enthalpy/free energy reaction coordinate profile for gold-catalyzed cyclization of diol **54** via the alkene−gold complex **58** is shown in Scheme 15. After **TS-1-*anti***, there is an endothermic intermediate **INT-2** with an enthalpy of 6.9 kcal/mol relative to the diol complex **58**. This intermediate has fully formed the C−O bond, and the hydrogen-bonding interaction between the hydroxyl groups becomes tighter with the distance between the allylic oxygen atom and the non-allylic hydroxyl group hydrogen atom reduced to 1.50 Å. However, the hydrogen atom has not been transferred between hydroxyl groups. This intermediate has also fully formed a C−Au bond at 2.14 Å and has almost completely ruptured the alkene π-bond, which is stretched to 1.49 Å.

dx.doi.org/10.1021/ja306333a | J. Am. Chem. Soc. 2012, 134, 16307−16318

Scheme 15. Enthalpy (Free Energy) Surface for Cyclization of Diol Complex (*E*)-58 (kcal/mol)

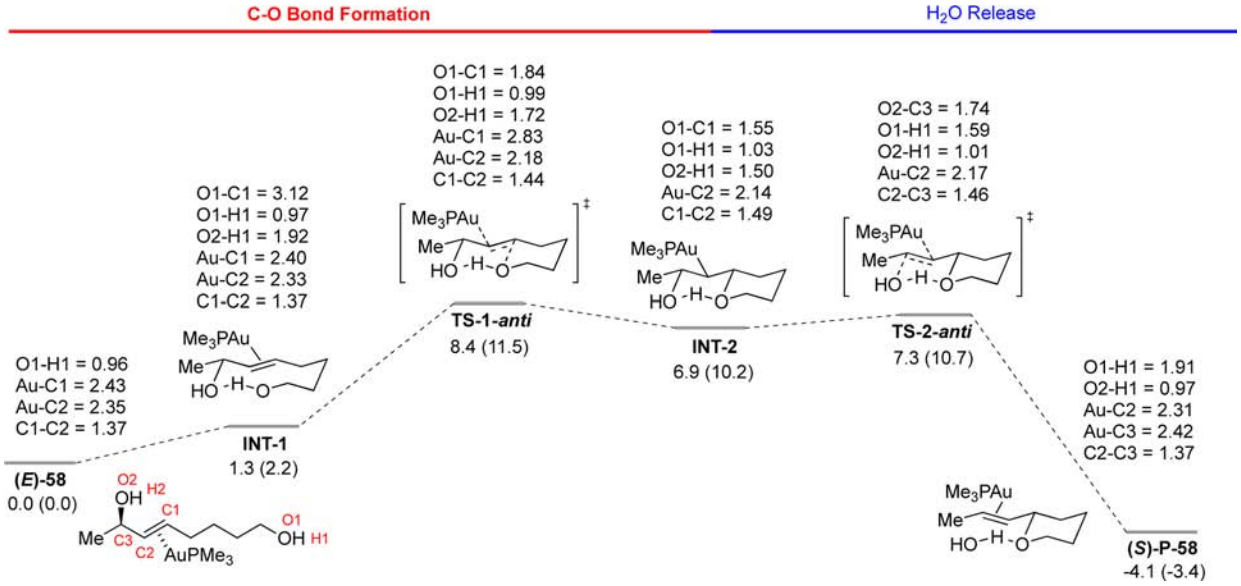

INT-2 resides in a very shallow well, and the barrier for concerted proton transfer and water release via **TS-2-*anti*** occurs with a $\Delta H^{\ddagger}$ and $\Delta G^{\ddagger}$ of 7.3 and 10.7 kcal/mol, respectively, relative to (*E*)-**58**. In **TS-2-*anti*** the breaking allylic C−O bond is stretched to 1.74 Å. The hydrogen is also transferred simultaneous to C−O bond cleavage, and this transfer is almost complete with a breaking O−H partial bond length of 1.59 Å and the forming O−H partial bond length of 1.01 Å. The resulting tetrahydropyran product, (*S*)-**P-58**, with cationic gold coordinated is exothermic by −4.1 kcal/mol and exergonic by −3.4 kcal/mol relative to Au diol complex (*E*)-**58**.

The reaction pathway outlined in Scheme 15 resembles the mechanism proposed by Paton and Maseras for Au-mediated intermolecular allylic ether isomerization.[30d] Our computed mechanism suggests that the rate-/turnover-determining transition state is **TS-1-*anti*** on the basis of this free energy surface. However, application of the energetic span model for catalytic cycles suggests that both **TS-1-*anti*** and **TS-2-*anti*** contribute to controlling the turnover frequency, due to their roughly equal transition-state heights.[31] At 298 K, the estimated turnover frequency is $\sim 10^4$ s^{-1} with **TS-1-*anti*** responsible for 0.8/1.0 of the turnover frequency dependency and **TS-2-*anti*** responsible for 0.2/1.0 of the turnover frequency.

TS-1-*anti* is also stereo-determining, as this transition state sets the tetrahydropyran stereocenter. In addition, **TS-1-*anti*** also ultimately determines alkene stereochemistry because the hydrogen-bonding interaction between diol groups is unlikely to be broken along the reaction pathway, and transformation of **INT-2** to the product via **TS-2-*anti*** is generally an irreversible step in the catalytic cycle.

In (*S*)-**P-58**, the expelled water remains in hydrogen bond contact with the tetrahydropyran. Importantly, the water produced in this reaction has the possibility to coordinate to the cationic $^{+}Au(PMe_3)$ to give $[(OH_2)Au(PMe_3)]^{+}$. Water coordination is ∼5 kcal/mol exothermic compared to (*S*)-**P-58**, suggesting that water poisons the electrophilic Au catalyst.

In the above calculations, PMe_3 was used in place of PPh_3, which is employed under the standard reaction conditions.[24] As a control experiment, the chirality transfer reaction was tested using Me_3PAuCl in place of the Ph_3PAuCl. As is shown in Scheme 16, the chirality was indeed transferred in the same sense and validates the use of PMe_3 as a computational model. We also note that we have employed a monomeric Au complex as a catalyst model. This is reasonable, considering that Gagné and Widenhoefer have recently shown that dimeric Au or Au/Ag complexes are likely to only play off-cycle roles.[32]

Scheme 16. Chirality Transfer Using Me_3PAuCl Precatalyst

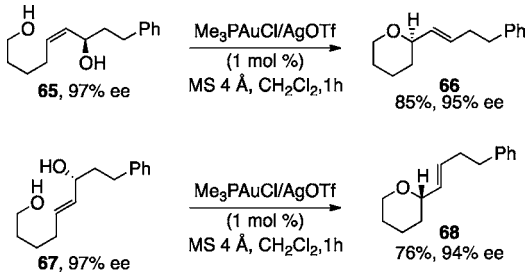

The dehydrative cyclization reaction of monoallylic diol **26** was also modeled (Scheme 17). This diol differs from diol **54** in that the methyl group is now replaced with a cyclohexyl group at the stereocenter and is an experimental system that has been shown to cyclize. The transition states and intermediates have nearly identical geometries, but the activation barriers are reduced by 2−3 kcal/mol.

Importantly, the mechanism outlined in Schemes 15 and 17 illustrates how the σ-Au intermediates **INT-2** and **INT-4** are not dead ends. Under many intramolecular cyclization conditions these intermediates would typically be unreactive toward protodeauration and severely hinder catalyst turnover. However, σ-Au intermediates **INT-2** and **INT-4** escape the need for gold−carbon σ-bond protodemetalation because of the available intramolecular proton transfer pathway between hydroxyl groups. This pathway allows efficient regeneration of the Au catalyst since water loss is facile.

Now that the lowest energy pathway for cyclization has been outlined, we are in position to explain why *anti*-alkoxyauration alkene addition is lower in energy than *syn*-alkoxyauration alkene addition. Three-dimensional representations of **TS-1-*syn*** and **TS-1alt-*syn*** are shown in Figure 4. The $\Delta H^{\ddagger}$ and $\Delta G^{\ddagger}$

dx.doi.org/10.1021/ja306333a | J. Am. Chem. Soc. 2012, 134, 16307−16318

Scheme 17. Enthalpy (Free Energy) Surface for Cyclization of Allylic Diol Complex (*E*)-69 (kcal/mol)

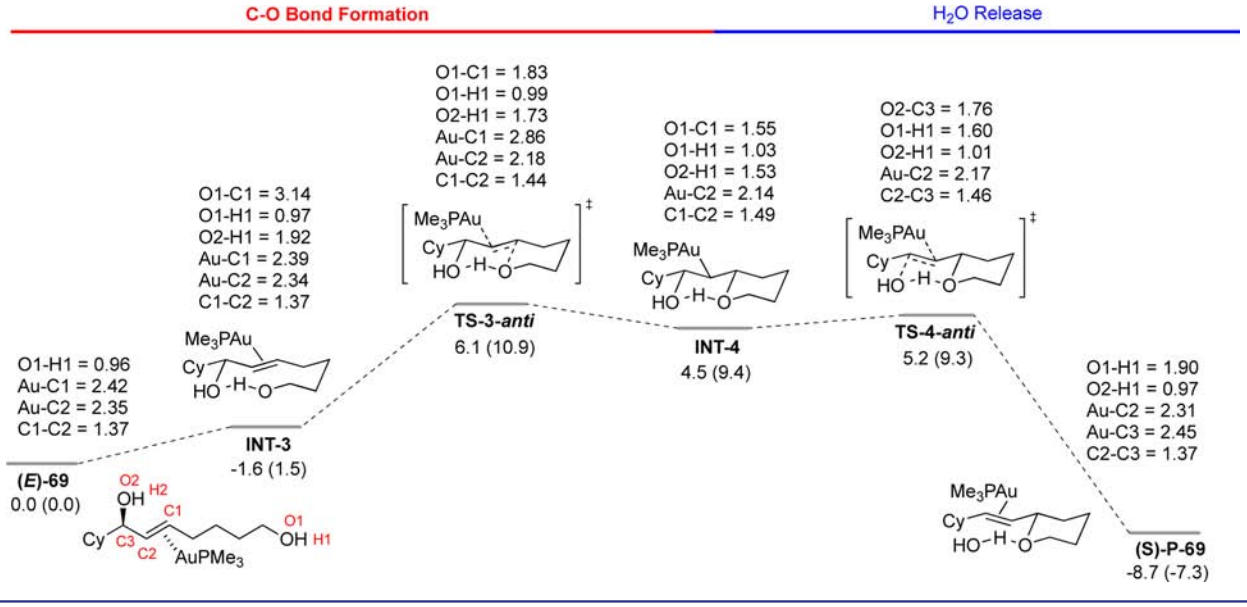

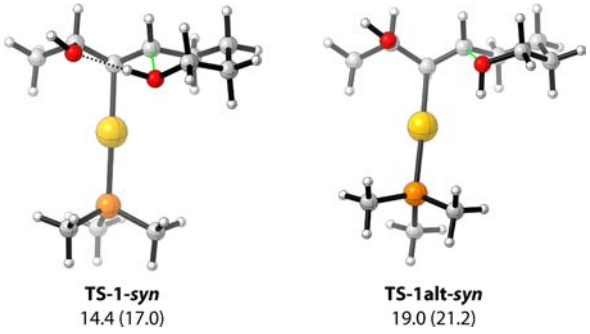

Figure 4. *syn*-Alkoxyauration alkene addition transition states. Enthalpies (free energies) are reported relative to gold diol complex (*E*)-**58** (kcal/mol).

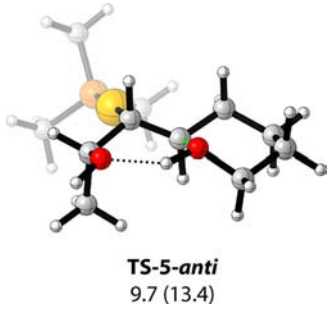

Figure 5. Lowest energy alkoxyauration alkene addition transition state leading to the non-observed tetrahydropyran diastereoisomer **57**. Enthalpy (free energy) reported relative to gold diol complex (*E*)-**58** (kcal/mol).

values for **TS-1-*syn*** are 14.4 and 17.0 kcal/mol, respectively, relative to gold-coordinated diol complex (*E*)-**58**. In this *syn*-addition transition state, the alkene-coordinated cationic $^{+}$Au(PMe$_3$) orients at a ∼45° dihedral angle relative to the forming C−O bond rather than a 90° dihedral angle that would be expected for true *syn*-addition. The Au(PMe$_3$) group twists out of the way to allow for the most favorable possible intramolecular hydrogen bonding between diol groups. In **TS-1-*syn*** the O···HO distance is 1.93 Å. This is about 0.1 Å longer than the hydrogen bond contact distance in **TS-1-*anti***. However, hydrogen bonding is not the only reason why this twisted geometry is adopted in the *syn*-transition state. When the hydrogen-bonding interaction is disconnected, the twisting remains. For example, in **TS-1alt-*syn*** (Figure 4), the non-allylic hydroxyl group is oriented so that the hydrogen-bonding interaction is severed, but the twisting of Au remains. This transition state has an activation barrier ∼5 kcal/mol higher than that of **TS-1-*syn***. It should be noted that all transition states without hydrogen bonding are higher in energy than the transition states that involve hydrogen bonding. The transition-state geometry of **TS-1alt-*syn*** suggests that the twisting is also the result of repulsion between the Au metal center and the hydroxyl groups.

To understand the stereoselectivity, we have also computed the lowest energy transition state that gives the unobserved diastereomer **57** (Scheme 12) of the tetrahydropyran product **55**. Figure 5 shows **TS-5-*anti*** that is the lowest energy transition state with the opposite tetrahydropyran stereocenter and *cis*-alkene configuration after water elimination. In **TS-5-*anti*** there is again hydrogen bonding between diol groups and *anti*-addition to the alkene, similar to that in **TS-1-*anti***. The $\Delta H^{\ddagger}$ and $\Delta G^{\ddagger}$ values for **TS-5-*anti*** are 9.7 and 13.4 kcal/mol, respectively, relative to the gold diol complex (*E*)-**58**. These barriers are 1.3 and 1.2 kcal/mol higher in enthalpy and free energy, respectively, than the barriers for **TS-1-*anti***. The geometry of **TS-5-*anti*** is nearly identical to that of **TS-1-*anti*** for the forming C−O bond and the hydrogen-bonding interactions. However, in **TS-5-*anti*** the methyl group at the allylic hydroxyl stereocenter is now in an axial position and results in allylic A$_{1,3}$ strain to achieve both hydrogen bonding between diol groups and *anti*-gold addition. Transition states leading to unobserved stereoisomers **56** and **44** are also higher in energy, since these transition states require disconnection of the intramolecular diol hydrogen bonding.

Since allylic A$_{1,3}$ strain, as a result of diol hydrogen bonding, controls the stereoselectivity of this reaction, replacement of the methyl group in **54** with a cyclohexyl group to give diol **26** results in an increase in the computed energy difference between the competing transition states. The free energy difference between **TS-3-*anti*** and the next lowest energy

dx.doi.org/10.1021/ja306333a | J. Am. Chem. Soc. 2012, 134, 16307−16318

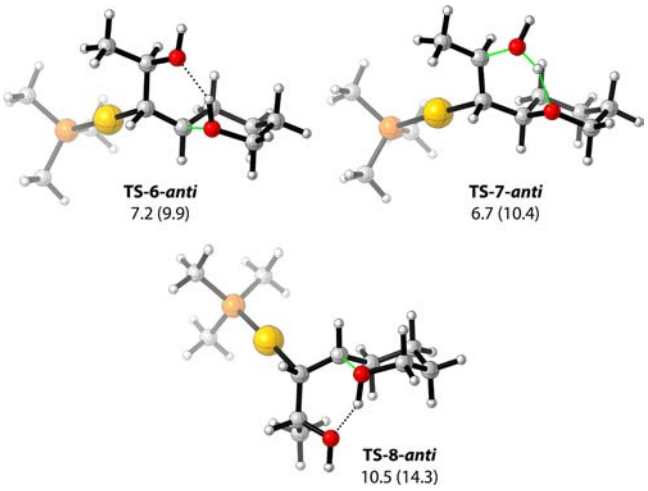

Figure 6. (Top) Lowest energy cyclization and water release transition states. (Bottom) Lowest energy transition state giving the unobserved stereoisomer for the *cis*-allylic diol. Enthalpies (free energies) reported relative to the ground-state gold *cis*-allylic diol complex (kcal/mol).

diastereomeric transition state for diol **26** is 2.3 kcal/mol, which corresponds to the greater than 20:1 ratio observed experimentally.

Experimentally, Scheme 9 and Figure 1 showed that the cyclizations of *cis*- and *trans*-allylic diols **34** and **35** are stereospecific. Computational analysis of a model *cis*-allylic diol revealed that the mechanistic pathway followed is highly similar to that for cyclization of **54**. Figure 6 shows the lowest energy transition state for Au-catalyzed cyclization and water release of the *cis*-allylic diol complex (*Z*)-**58**.

TS-6-*anti* again shows that *anti*-addition is most favorable compared to *syn*-addition or concerted addition. The main difference between **TS-6-*anti*** and **TS-1-*anti*** is that, to allow for the intramolecular diol hydrogen-bonding interaction, the *cis*-allylic diol adopts a *cis*-decalin-like geometry, whereas the *trans*-allylic diol transition state adopts a *trans*-decalin-like geometry. Again, the reaction stereoselectivity is controlled by this intramolecular hydrogen-bonding interaction. Another difference is that the water release transition state **TS-7-*anti*** is slightly higher in free energy than the cyclization transition state.

Figure 6 also shows transition state **TS-8-*anti*** that results in an unobserved stereoisomer from cyclization of the *cis*-allylic diol. Similar to the cyclization of the *trans*-allylic diol, allylic $A_{1,3}$ strain-type interactions result in **TS-8-*anti*** having a 4.4 kcal/mol higher free energy barrier than **TS-6-*anti*** and a 3.9 kcal/mol higher free energy barrier than **TS-7-*anti***. The calculated free energy surface for this pathway is included as Scheme 18.

Table 1. Leaving Group Effects

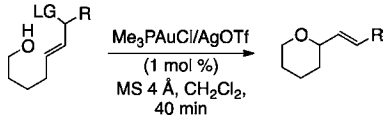

entry	leaving group	R	yield (%)
1	OH	C_6H_{11}	96[a]
2	OTBS	C_6H_{11}	12[a]
3	OMe	C_6H_{11}	9[a,c]
4	OAc	C_6H_{11}	<5[b]
5	Cl	H	0[b]

[a]Isolated yield. [b]Yield determined by ^{1}H NMR, 500 MHz. [c]69% isolated yield with 18% recovered starting material when the reaction was allowed to stir for 48 h.

To probe the potential hydrogen-bonding effects and possibility for chemoselectivity in synthetic applications, the nature of the leaving group was varied (Table 1). Interestingly, when the traditional leaving group ability is increased, the yield of the reaction decreases, as evidenced by the hydroxyl group providing by far the best conversion and yield (entry 1). Conversion can be improved with longer reaction times, and with a methoxy leaving group, the product could be isolated in 69% yield with 18% of the starting material recovered if the reaction was allowed to stir for 48 h (entry 3, footnote *c*). These ether substrates were also tested in chirality transfer

Scheme 18. Enthalpy (Free Energy) Surface for Cyclization of *cis*-Allylic Diol Complex (*Z*)-58 (kcal/mol)

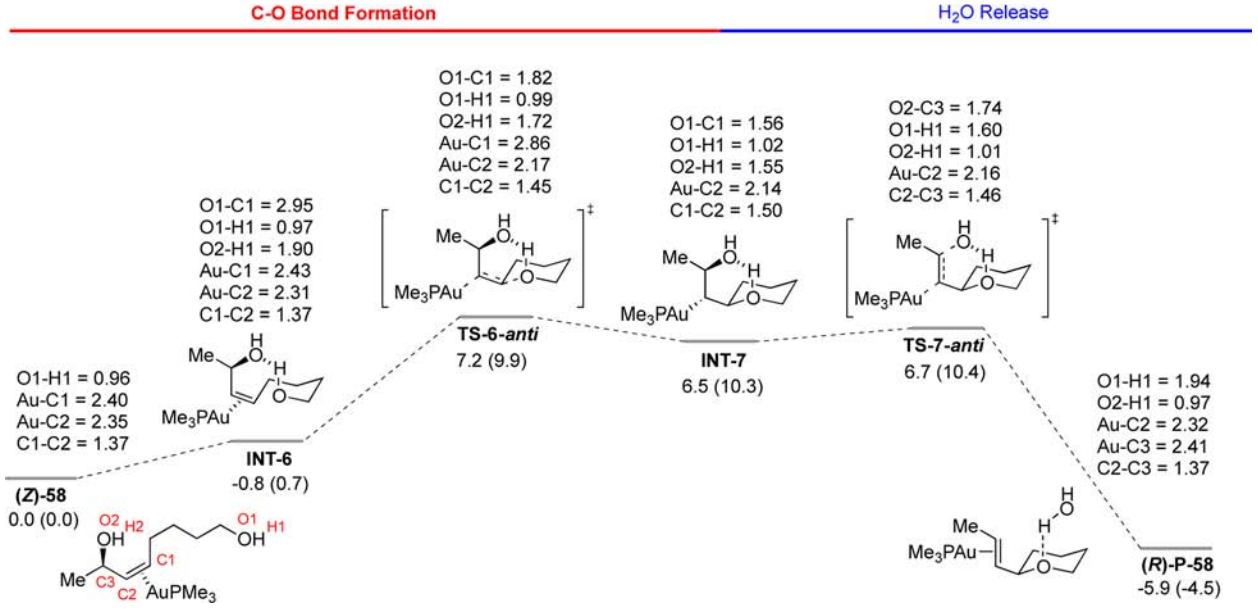

dx.doi.org/10.1021/ja306333a | J. Am. Chem. Soc. 2012, 134, 16307−16318

experiments (Scheme 19). Using the standard conditions, but with higher catalyst loadings (5 mol %), after 2 h the

Scheme 19. Chirality Transfer with Methyl Ether Leaving Groups

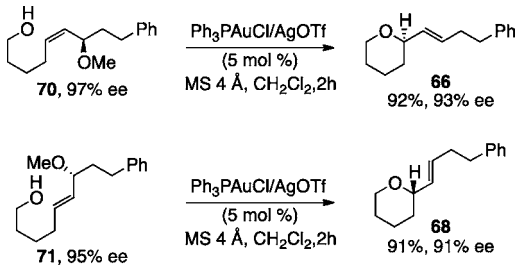

tetrahydropyran products were obtained in high yield, and the chirality was efficiently transferred with the same sense of chirality as the standard substrates. This efficient chirality transfer, albeit a slower reaction, is also consistent with the proposed hydrogen bonding in the transition state.

The observed yields (Table 1) appear to correlate with a nearly inverse relationship to leaving group ability. Stated in another way, the reaction proceeds best with electron-rich leaving groups. This phenomenon was studied computationally with acetate as a leaving group, and it was found that the activation barriers for alkoxyauration and elimination both increase. Figure 7 shows the lowest energy cyclization transition

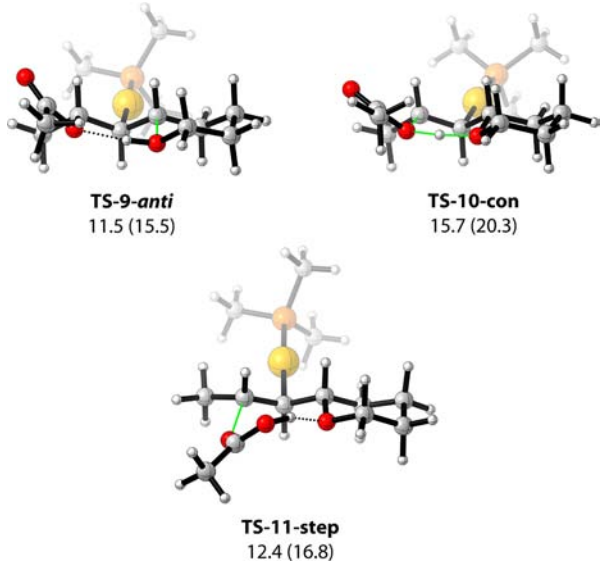

Figure 7. Alkoxyauration and acetic acid elimination transition states for the substrate bearing an acetate leaving group (Table 1). Enthalpies (free energies) are reported relative to the ground-state gold alkene complex (kcal/mol).

state and both stepwise and concerted HOAc release transition states. The *anti*-addition transition state, **TS-9-*anti***, has $\Delta H^{\ddagger}$ and $\Delta G^{\ddagger}$ values of 11.5 and 15.5 kcal/mol, which are 3.1 and 4.0 kcal/mol higher than the barrier found for **TS-1-*anti***. The larger barrier for **TS-9-*anti*** is the result of the poor hydrogen-bonding acceptor ability of the OAc group compared with a hydroxyl group. This results in the hydroxyl group participating in C−O bond formation of the tetrahydropyran being less nucleophilic.

Unlike the reaction mechanism of allylic diols, where proton transfer and water release occur in the same step, the lowest energy pathway for turnover of the σ-Au intermediate formed from **TS-9-*anti*** occurs in two steps, where there is a discrete proton transfer that occurs prior to HOAc group dissociation via **TS-11-step**. This pathway, with an activation enthalpy of 12.4 kcal/mol, is 3.3 kcal/mol lower in energy than the concerted proton transfer and HOAc release via **TS-10-con**. Interestingly, the poor leaving group ability of HOAc, compared to H_2O, results in **TS-10-step** becoming turnover frequency determining rather than the *anti*-addition transition state **TS-9-*anti***.

These results again highlight the need for a facile route for turnover of the σ-Au intermediate generated from intramolecular cyclization. When proton transfer occurs between hydroxyl groups, water is efficiently expelled. However, proton transfer to a group such OAc leads to a much less efficient expulsion of HOAc and much slower turnover of the σ-Au intermediate.

As described above (Scheme 11, Figure 2), Robertson and co-workers have reported gold-catalyzed cyclization of monoallylic diols **45**, **48**, and **50** that give tetrahydrofurans **46**, **47**, **49**, and **51**.[18] Interestingly, the observation of a ∼2:1 mixture of tetrahydrofurans **46** and **47** is in contrast to the cyclization of diols reported by Aponick and co-workers that gave only one stereoisomeric product with respect to both the geometry of the newly formed olefin and the stereocenter.[24] Additionally, while **48** and **50** afforded only the predicted *trans*-olefin products, the sense of chirality transfer for cyclization of **45** was opposite to that observed previously in Aponick's examples involving tetrahydropyrans. These results were quite thought-provoking, and the mechanism for this system was also studied computationally.

For monoallylic diols **45**, **48**, and **50**, the lowest energy pathway for cyclization again involves stepwise *anti*-addition. The C−O bond formation and proton transfer/water release transition states **TS-12-*anti*** and **TS-13-*anti*** lead to the alkene **46**, while **TS-14-*anti*** and **TS-15-*anti*** give the *trans*-alkene **47**. Inspection of transition states **TS-12-*anti*/TS-13-*anti*** and **TS-14-*anti*/TS-15-*anti*** reveals why they are competitive (Figure 8). On the basis of the stereoselectivity for the Aponick systems, one would expect **TS-12-*anti*** and **TS-13-*anti*** to be favored over **TS-14-*anti*** and **TS-15-*anti*** since there is a lack of allylic 1,3-strain. However, the forming tetrahydrofuran ring system adopts a conformation that orients the phenyl group in a pseudoaxial position. In contrast, in **TS-14-*anti*** and **TS-15-*anti***, there is allylic 1,3-strain, but the phenyl group is oriented in an equatorial position on the forming tetrahydrofuran ring. As a result of these competing effects, there is no significant diastereomeric preference for cyclization of diol **45**. In contrast, in the transition states for the cyclization of diols **48** and **50**, these effects are additive to give high stereoselectivity.

The complete enthalpy/free energy surface for Au-catalyzed cyclization of **45** to **46** is shown in Scheme 20. On the basis of the free energies, the energetic span model[31] assigns **TS-13-*anti***, with $\Delta G^{\ddagger}$ = 15.6 kcal/mol, to be turnover frequency determining by 0.7/1.0, and **TS-12-*anti***, with $\Delta G^{\ddagger}$ = 15.1 kcal/mol, to be turnover frequency determining by 0.3/1.0.

For generation of the alternative diastereoisomer, the $\Delta G^{\ddagger}$ for **TS-15-*anti*** is 19.0 kcal/mol. Unfortunately, the free energy difference between **TS-13-*anti*** and **TS-15-*anti*** is overestimated since the experimental ratio of **46**:**47** is ∼2:1.

dx.doi.org/10.1021/ja306333a | J. Am. Chem. Soc. 2012, 134, 16307−16318

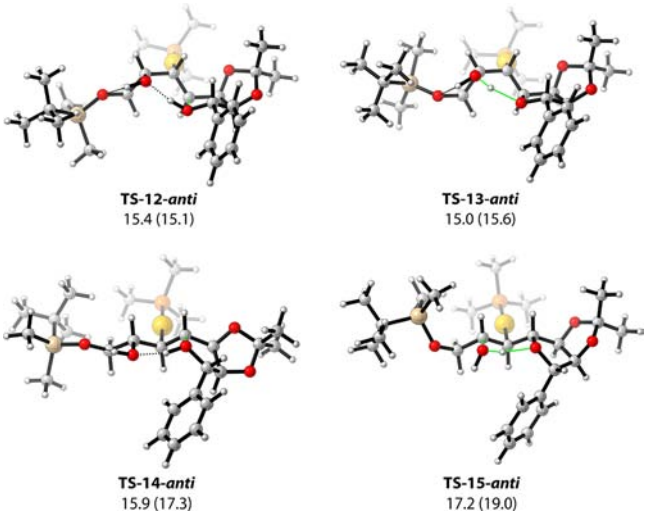

Figure 8. Alkoxyauration and water release transition states for monoallylic diol **45**. Enthalpies (free energies) are reported relative to the ground-state gold diol complex of compound **45** (kcal/mol).

While these data are consistent, in light of Robertson's suggestive mnemonic (Figure 2), further experimental data on the *syn*- versus *anti*-addition and the importance of hydrogen bonding were collected using bicyclic systems **73**−**75** (Figure 9). As is shown in Figure 9, the reactivity was predicted to increase from **73** to **75** on the basis of the ability to hydrogen bond and the accessibility of the correct olefin π-face for *anti*-alkoxyauration. While **73** cannot achieve the geometry necessary for hydrogen bonding, **74** and **75** would be predicted to easily attain the required conformation. With these compounds, *anti*-alkoxyauration should be much more readily accomplished upon complex formation with **75**, as the *exo*-π-face should be readily accessible in comparison to the requisite *endo*-π-face in **74**.

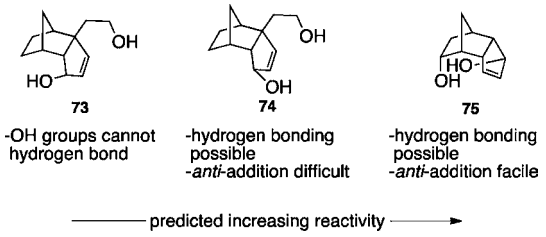

Figure 9. Bicyclic systems as mechanistic probes.

Scheme 21. Au-Catalyzed Cyclization of Bicyclic Diols

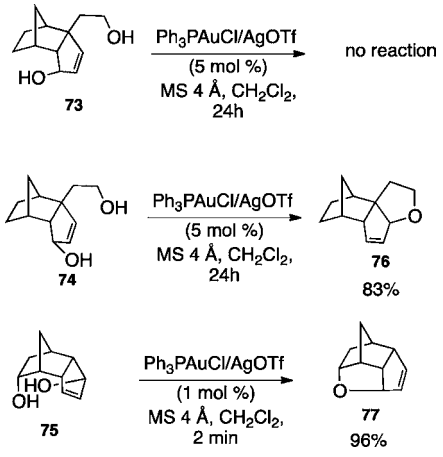

In the event, the predicted reactivities were borne out. As can be seen in Scheme 21, upon exposure of **73** to the standard reaction conditions, with the exception of increased catalyst loading (5 mol %), no reaction was observed. In contrast, diastereomer **74** underwent slow conversion to yield **76** in 83% after 24 h, and an extremely rapid reaction was observed for **75**.

Scheme 20. Enthalpy (Free Energy) Surface for Cyclization of Monoallylic Diol 45 (kcal/mol)

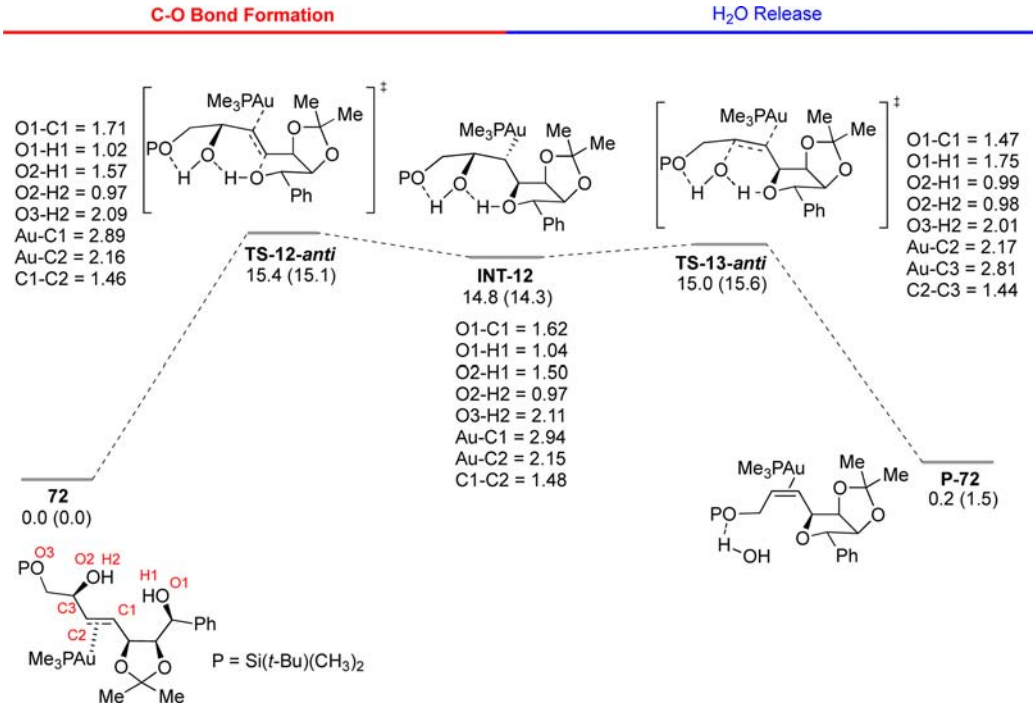

dx.doi.org/10.1021/ja306333a | J. Am. Chem. Soc. 2012, 134, 16307−16318

Using 1 mol % catalyst, **75** provided **77** in 96% yield after a 2 min reaction time.

Computational modeling of bicyclic systems **73**–**75**, which was performed prior to experiment, is consistent with the observed experimental reactivity. No *anti*-addition transition state was located for **73** due to the absence of hydrogen-bonding interactions. For bicycles **74** and **75**, the *anti*-addition transition states are shown in Figure 10. **TS-16-*anti*** that

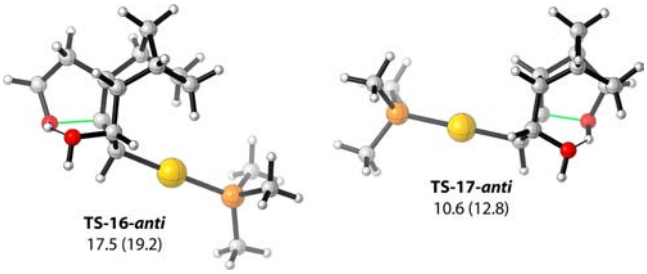

Figure 10. *anti*-Addition transition states for bicycles **74** and **75** (kcal/mol). Energies relative to the Au-alkene complex.

corresponds to cyclization of **74** has an activation enthalpy of 17.5 kcal/mol. This is significantly higher than the 8.4 kcal/mol activation enthalpy found for **TS-1-*anti*** for the acyclic system and consistent with the lower yield and longer reaction time. In contrast, **TS-17-*anti*** that corresponds to cyclization of **75** has an activation enthalpy of only 10.6 kcal/mol due to ideal hydrogen bonding and the ability for the Au catalyst to coordinate to the non-hindered *exo*-π-face, resulting in a facile cyclization process.

CONCLUSIONS

In summary, mechanistic studies highlight the importance of hydrogen bonding in the Au-catalyzed cyclization of allylic diols. After extensive DFT calculations and further experiments on substrates designed to probe the reaction mechanism, cationic and concerted S_N2'-like pathways can effectively be ruled out, and a two-step *anti*-alkoxyauration/*anti*-elimination mechanism, consistent with all data observed to date, is proposed. This pathway relies on hydrogen bonding to not only template the stereochemistry of the reaction but also accelerate the rate by increasing the leaving group ability of the hydroxyl group and obviating the need for intermolecular proton transfer steps. The reaction is a further demonstration that pathways alternative to protodeauration can readily be achieved and lead to highly useful reaction products.

ASSOCIATED CONTENT

Supporting Information

Experimental procedures and characterization data for new compounds, complete ref 19, and xyz coordinates. This material is available free of charge via the Internet at http://pubs.acs.org.

AUTHOR INFORMATION

Corresponding Author

aponick@chem.ufl.edu; dhe@chem.byu.edu

Notes

The authors declare no competing financial interest.

ACKNOWLEDGMENTS

D.H.E. thanks Brigham Young University (BYU) and the Fulton Supercomputing Lab for computational support. B.H.K. thanks the BYU Department of Chemistry and Biochemistry for an undergraduate research award. A.A. thanks the Herman Frasch Foundation (647-HF07), the James and Ester King Biomedical Research Program (09KN-01), and Petra Research, Inc. for their generous support of our programs.

REFERENCES

(1) For recent reviews on Au catalysis, see: (a) Rudolph, M.; Hashmi, A. S. K. *Chem. Commun.* **2011**, *47*, 6536–6544. (b) Corma, A.; Leyva-Pèrez, A.; Sabater, M. J. *Chem. Rev.* **2011**, *111*, 1657–1712. (c) Hashmi, A. S. K.; Buhrle, M. *Aldrichim. Acta* **2010**, *43*, 27–33. (d) Hashmi, A. S. K. *Angew. Chem., Int. Ed.* **2010**, *49*, 5232–5241. (e) Shapiro, N. D.; Toste, F. D. *Synlett* **2010**, 675–691. (f) Hashmi, A. S. K.; Rudolph, M. *Chem. Soc. Rev.* **2008**, *37*, 1766–1775. (g) Li, Z.; Brouwer, C.; He, C. *Chem. Rev.* **2008**, *108*, 3239–3265. (h) Arcadi, A. *Chem. Rev.* **2008**, *108*, 3366–3325. (i) Gorin, D. J.; Sherry, B. D.; Toste, F. D. *Chem. Rev.* **2008**, *108*, 3351–3378. (j) Muzart, J. *Tetrahedron* **2008**, *64*, 5815–5849. (k) Shen, H. C. *Tetrahedron* **2008**, *64*, 3885–3903.

(2) Teles, J. H.; Brode, S.; Chabanas, M. *Angew. Chem., Int. Ed.* **1998**, *37*, 1415–1417.

(3) For allenes, see: (a) Winter, C.; Krause, N. *Chem. Rev.* **2011**, *111*, 1994–2009 and references therein. For select examples of addition to alkenes, see: (b) Zhang, J.; Yang, C.-G.; He, C. *J. Am. Chem. Soc.* **2006**, *128*, 1798–1799. (c) Han, X.; Widenhoefer, R. A. *Angew. Chem., Int. Ed.* **2006**, *45*, 1747–1749. (d) Zhang, Z.; Lee, S. D.; Widenhoefer, R. A. *J. Am. Chem. Soc.* **2009**, *131*, 5372–5373. (e) Wang, M.-Z.; Wong, M.-K.; Che, C.-M. *Chem.–Eur. J.* **2008**, *14*, 8353–8364. (f) Kovács, G.; Lledós, A.; Ujaque, G. *Organometallics* **2010**, *29*, 3252–3260 and references therein.

(4) For Au catalysis, see: (a) Hashmi, A. S. K. *Catal. Today* **2007**, *122*, 211–214. (b) McKinney, R. E. M.; Widenhoefer, R. A. *Chem.—Eur. J.* **2011**, 6170–6178. For studies on protic acid being the true catalyst with a variety of metals, see: (c) Rosenfeld, D. C.; Shekhar, S.; Takemiya, A.; Utsunomiya, M.; Hartwig, J. F. *Org. Lett.* **2006**, *8*, 4179–4182. (d) Taylor, J. G.; Adrio, L. A.; Hii, K. K. *Dalton Trans.* **2010**, *39*, 1171–1175. (e) Adrio, L. A.; Quek, L. S.; Taylor, J. G.; Hii, K. K. *Tetrahedron* **2009**, *65*, 10334–10338. (f) McBee, J. L.; Bell, A. T.; Tilley, T. D. *J. Am. Chem. Soc.* **2008**, *130*, 16562–16571. (g) Cheng, X.; Xia, Y.; Wei, H.; Xu, B.; Zhang, C.; Li, Y.; Qian, G.; Zhang, X.; Li, K.; Li, W. *Eur. J. Org. Chem.* **2008**, 1929–1936. (h) Wabnitz, T. C.; Yu, J. Q.; Spencer, J. B. *Chem.—Eur. J.* **2004**, *10*, 484–493.

(5) (a) Antoniotti, S.; Genin, E.; Michelet, V.; Genêt, J.-P. *J. Am. Chem. Soc.* **2005**, *127*, 9976–9977. (b) Zhang, Z.; Liu, C.; Kinder, R. E.; Han, X.; Qian, H.; Widenhoefer, R. A. *J. Am. Chem. Soc.* **2006**, *128*, 9066–9073. (c) Yang, C.-G.; He, C. *J. Am. Chem. Soc.* **2005**, *127*, 6966–6967.

(6) For a review on the isolation of organogold complexes, see: Liu, L.-P.; Hammond, G. B. *Chem. Soc. Rev.* **2012**, *41*, 3129–3139.

(7) Lalonde, R. L.; Brenzovich, W. E., Jr.; Benitez, D.; Tkatchouk, E.; Keley, K.; Goddard, W. A.; Toste, F. D. *Chem. Sci.* **2010**, *1*, 226–233.

(8) (a) Li, S.; Li, Z.; Yuan, Y.; Peng, D.; Li, Y.; Zhang, L.; Wu, Y. *Org. Lett.* **2012**, *14*, 1130–1133. (b) Leyva-Perez, A.; Doménech, A.; Al-Resayes, S. I.; Corma, A. *ACS Catal.* **2012**, *2*, 121–126. (c) Hopkinson, M. N.; Gee, A. D.; Gouverner, V. *Chem. –Eur. J.* **2011**, *17*, 824–8262. (d) Zhang, G.; Luo, Y.; Wang, Y.; Zhang, L. *Angew. Chem., Int. Ed.* **2011**, *50*, 4450–4454. (e) Tkatchouk, E.; Mankad, N. P.; Benitez, D.; Goddard, W. A.; Toste, F. D. *J. Am. Chem. Soc.* **2011**, *133*, 14293–14300. (f) de Haro, T.; Nevado, C. *Angew. Chem., Int. Ed.* **2011**, *50*, 906–910. (g) Brenzovich, W. E., Jr.; Brazeau, J.-F.; Toste, F. D. *Org. Lett.* **2010**, *12*, 4728–4731. (h) Mankad, N. P.; Toste, F. D. *J. Am. Chem. Soc.* **2010**, *132*, 12859–12861. (i) Melhado, A. D.; Brenzovich, W. E.; Lackner, A. D.; Toste, F. D. *J. Am. Chem. Soc.* **2010**, *132*, 8885–8887. (j) Brenzovich, W. E., Jr.; Benitez, D.; Lackner, A. D.;

Shunatona, H. P.; Tkatchouk, E.; Goddard, W. A.; Toste, F. D. *Angew. Chem., Int. Ed.* **2010**, *49*, 5519−5522. (k) Ball, L. T.; Green, M.; Lloyd-Jones, G. C.; Russell, C. A. *Org. Lett.* **2010**, *12*, 4724−4727. (l) Hopkinson, M. N.; Tessier, A.; Salisbury, A.; Giuffredi, G. T.; Combettes, L. E.; Gee, A. D.; Gouverneur, V. *Chem.—Eur. J.* **2010**, *16*, 4739−4743. (m) Zhang, G.; Peng, Y.; Cui, L.; Zhang, L. *Angew. Chem., Int. Ed.* **2009**, *48*, 3112−3115. (n) Hashmi, A. S. K.; Ramamurthi, T. D.; Rominger, F. *J. Organomet. Chem.* **2009**, *694*, 592−597. (o) Wegner, H. A.; Ahles, S.; Neuburger, M. *Chem.—Eur. J.* **2008**, *14*, 11310−11313. (p) Hashmi, A. S. K.; Blanco, M. C.; Fischer, D.; Bats, J. W. *Eur. J. Org. Chem.* **2006**, 1387−1389.

(9) (a) Mankad, N. P.; Toste, F. D. *Chem. Sci.* **2012**, *3*, 72−76. (b) Zhang, G.; Cui, L.; Wang, Y.; Zhang, L. *J. Am. Chem. Soc.* **2010**, *132*, 1474−1475. (c) Iglesias, A.; Muńiz, K. *Chem.—Eur. J.* **2009**, *15*, 10563−10569.

(10) (a) Aponick, A.; Li, C.-Y.; Biannic, B. A. *Org. Lett.* **2008**, *10*, 669−671. (b) Aponick, A.; Biannic, B. *Synthesis* **2008**, *20*, 3356−3359.

(11) For leading references, see: (a) Wang, Z. J.; Benitez, D.; Tkatchouk, E.; Goddard, W. A., III; Toste, F. D. *J. Am. Chem. Soc.* **2010**, *132*, 13064−13071. (b) LaLonde, R. L.; Wang, Z. J.; Mba, M.; Lackner, A. D.; Toste, F. D. *Angew. Chem., Int. Ed.* **2010**, *49*, 598−601. (c) Zhang, Z.; Widenhoefer, R. A. *Angew. Chem., Int. Ed.* **2007**, *46*, 283−285. (d) Hamilton, G. L.; Kang, E. J.; Mba, M.; Toste, F. D. *Science* **2007**, *317*, 496−499.

(12) (a) Biannic, B.; Aponick, A. *Eur. J. Org. Chem.* **2011**, 6605−6617. (b) Aponick, A.; Li, C.-Y.; Palmes, J. A. *Org. Lett.* **2009**, *11*, 121−124. (c) Aponick, A.; Li, C.-Y.; Malinge, J.; Marques, E. F. *Org. Lett.* **2009**, *11*, 4624−4627. (d) Aponick, A.; Biannic, B; Jong, M. R. *Chem. Commun.* **2010**, *46*, 6849−6851. (e) Mukherjee, P.; Widenhoefer, R. A. *Angew. Chem., Int. Ed.* **2012**, *49*, 1405−1407. (f) Mukherjee, P.; Widenhoefer, R. A. *Org. Lett.* **2011**, *13*, 1334−1337. (g) Mukherjee, P.; Widenhoefer, R. A. *Org. Lett.* **2010**, *12*, 1184−1187. (h) Bandini, M.; Eichholzer, A. *Angew. Chem., Int. Ed.* **2009**, *48*, 9533−9537. (i) Bandini, M.; Monari, M.; Romaniello, A.; Tragni, M. *Chem.—Eur. J.* **2010**, *16*, 14272−14277.

(13) Other metal-based catalysts have also been employed in substitution reactions of allylic alcohols. For leading references, see: (a) Satoh, T.; Ikeda, M.; Miura, M.; Nomura, M. *J. Org. Chem.* **1997**, *62*, 4877−4879. (b) Yang, S.-C.; Tsai, Y.-C. *Organometallics* **2001**, *20*, 763−770. (c) Ozawa, F.; Okamoto, H.; Kawagishi, S.; Yamamoto, S.; Minami, T.; Yoshifuji, M. *J. Am. Chem. Soc.* **2002**, *124*, 10968−10969. (d) Kinoshita, H.; Shinokubo, H.; Oshima, K. *Org. Lett.* **2004**, *6*, 4085−4088. (e) Uenishi, J.; Ohmi, M.; Ueda, A. *Tetrahedron: Asymmetry* **2005**, *16*, 1299−1303. (f) Kawai, N.; Lagrange, J.-M.; Ohmi, M.; Uenishi, J. *J. Org. Chem.* **2006**, *71*, 4530−4537. (g) Kawai, N.; Lagrange, J.-M.; Uenishi, J. *Eur. J. Org. Chem.* **2007**, 2808−2814. (h) Uenishi, J.; Vikhe, Y. S.; Kawai, N. *Chem.—Asian J.* **2008**, *3*, 473−484. (i) Utsunomiya, M.; Miyamoto, Y.; Ipposhi, J.; Ohshima, T.; Mashima, K. *Org. Lett.* **2007**, *9*, 3371−3374. (j) Mora, G.; Piechaczyk, O.; Houdard, R.; Mézailles, N.; Le Goff, X.-F.; Le Floch, P. *Chem.—Eur. J.* **2008**, *14*, 10047−10057. (k) Ohshima, T.; Miyamoto, Y.; Yasuhito, J.; Nakahara, Y.; Utsunomiya, M.; Mashima, K. *J. Am. Chem. Soc.* **2009**, *131*, 14317−14328. (l) Kabalka, G. W.; Dong, G.; Venkataiah, B. *Org. Lett.* **2003**, *5*, 893−895. (m) Zaitsev, A. B.; Gruber, S.; Plüss, P. A.; Pregosin, P. S.; Veiros, Wörle, M. *J. Am. Chem. Soc.* **2008**, *130*, 11604−11605. (n) van Rijn, J. A.; Lutz, M.; von Chrzanowski, L. S.; Spek, L. A.; Bouwman, E.; Drent, E. *Adv. Synth. Catal.* **2009**, *351*, 1637−1647. (o) Tanaka, S.; Seki, T.; Kitamura, M. *Angew. Chem., Int. Ed.* **2009**, *48*, 8948−8951. (p) Guérinot, A.; Serra-Muns, A.; Gnamm, C.; Bensoussan, C.; Reymond, S.; Cossy, J. *Org. Lett.* **2010**, *12*, 1808−1811. (q) Qin, H.; Yamagiwa, N.; Matsunaga, S.; Shibasaki, M. *Angew. Chem., Int. Ed.* **2007**, *46*, 409−413. (r) Lafrance, M.; Roggen, M.; Carreira, E. M. *Angew. Chem., Int. Ed.* **2012**, *51*, 3470−3473. (s) Miyata, K.; Katsuna, H.; Kawakami, S.; Kitamura, M. *Angew. Chem., Int. Ed.* **2011**, *50*, 4649−4653. (t) Miyata, K.; Kitamura, M. *Synthesis* **2012**, *44*, 2138−2146.

(14) Yang, C.-G.; He, C. *J. Am. Chem. Soc.* **2005**, *127*, 6966−6967.

(15) During optimization studies, reaction at −78 °C was observed but conversion was very slow. To achieve a balance of selectivity and reactivity, reactions at −50 °C were reported in ref 10.

(16) Komiya, S.; Ozaki, S. *Chem. Lett.* **1988**, *17*, 1431−1432.

(17) Guerinot, A.; Serra-Muns, A.; Bensiussan, C.; Reymond, S.; Cossy, J. *Tetrahedron* **2011**, *67*, 5024.

(18) Unsworth, W. P.; Stevens, K.; Lamont, S. G.; Robertson, J. *Chem. Commun.* **2011**, *47*, 7659−7661.

(19) Frisch, M. J.; et al. *Gaussian 09*, revision A.02; Gaussian, Inc.: Wallingford, CT, 2009.

(20) (a) Zhao, Y.; Truhlar, D. G. *Theor. Chem. Acc.* **2008**, *120*, 215−241. (b) Zhao, Y.; Truhlar, D. G. *Acc. Chem. Res.* **2008**, *41*, 157−167.

(21) Marenich, A. V.; Cramer, C. J.; Truhlar, D. G. *J. Phys. Chem. B* **2009**, *113*, 6378−6396.

(22) For leading references, see: (a) Jagdale, A. R.; Park, J. H.; Youn, S. W. *J. Org. Chem.* **2011**, *76*, 7204−7215. (b) Dombray, T.; Blanc, A.; Weibel, J.; Pale, P. *Org. Lett.* **2010**, *12*, 5362−5365. (c) Lin, C.-C.; Teng, T.-M.; Tsai, C.-C.; Liao, H.-Y.; Liu, R.-S. *J. Am. Chem. Soc.* **2008**, *130*, 16417−16423. (d) Dudnik, A. S.; Sromek, A. W.; Rubina, M.; Kim, J. T.; Kel'in, A. V.; Gevorgyan, V. *J. Am. Chem. Soc.* **2008**, *130*, 1440−1452. (e) Lin, C.-C.; Teng, T.-M.; Odedra, A.; Liu, R.-S. *J. Am. Chem. Soc.* **2007**, *129*, 3798−3799. (f) Sromek, A. W.; Rubina, M.; Gevorgyan, V. *J. Am. Chem. Soc.* **2005**, *127*, 10500−10501.

(23) (a) Gómez-Suárez, A.; Ramón, R. S.; Slawin, A. M. Z.; Nolan, S. P. *Dalton Trans.* **2012**, *41*, 5461−5463. (b) Ramón, R. S.; Gaillard, S.; Poater, A.; Cavallo, L.; Slawin, A. M. Z.; Nolan, S. P. *Chem.—Eur. J.* **2011**, *17*, 1238−1246. (c) Gaillard, S.; Slawin, A. M. Z.; Nolan, S. P. *Chem. Commun.* **2010**, *46*, 2742−2744.

(24) Aponick, A.; Biannic, B. *Org. Lett.* **2011**, *13*, 1330−1333.

(25) For reviews, see: (a) Magid, R. M. *Tetrahedron* **1980**, *36*, 1901−1930. (b) Paquette, L. A.; Stirling, C. J. M. *Tetrahedron* **1992**, *48*, 7383−7423.

(26) Streitwieser, A.; Jayasree, E. G.; Hasanayn, J.; Leung, S. S.-H. *J. Org. Chem.* **2008**, *73*, 9426−9434.

(27) (a) Gimeno, M. C.; Laguna, A. *Chem. Rev.* **1997**, *97*, 511−522. (b) Schulte, P.; Behrens, U. *Chem. Commun.* **1998**, 1633−1634. (c) Flores, J. A.; Dias, H. V. R. *Inorg. Chem.* **2008**, *47*, 4448−4450. (d) Dias, H. V. R.; Fianchini, M.; Cundari, T. R.; Campana, C. F. *Angew. Chem., Int. Ed.* **2008**, *47*, 556−559. (e) Carvajal, M. G.; Novoa, J. J.; Alvarez, S. *J. Am. Chem. Soc.* **2004**, *126*, 1465−1477. (f) Schwerdtfeger, P.; Hermann, H. L.; Schmidbaur, H. *Inorg. Chem.* **2003**, *42*, 1334−1342.

(28) For leading references, see: (a) Fañanás-Mastral, M.; Aznar, F. *Organometallics* **2009**, *28*, 666−668. (b) Frémont, P.; Marion, N.; Nolan, S. P. *J. Organomet. Chem.* **2009**, *694*, 551−560. (c) Wu, J.; Kroll, P.; Dias, H. V. R. *Inorg. Chem.* **2009**, *48*, 423−425. (d) Brown, T. J.; Dickens, M. G.; Widenhoefer, R. A. *Chem. Commun.* **2009**, 6451−6453. (e) Hooper, T. N.; Green, M.; McGrady, J. E.; Patel, J. R.; Russell, C. A. *Chem. Commun.* **2009**, 3877−3879. (f) Liu, L.-P.; Xu, B.; Mashuta, M. S.; Hammond, G. B. *J. Am. Chem. Soc.* **2008**, *130*, 17642−17643. (g) Shapiro, N. D.; Toste, F. D. *Proc. Natl. Acad. Sci. U.S.A.* **2008**, *105*, 2779−2782. (h) Lavallo, V.; Frey, G. D.; Donnadieu, B.; Soleilhavoup, M.; Bertrand, G. *Angew. Chem., Int. Ed.* **2008**, *47*, 5224−5228. (i) Fürstner, A.; Alcarazo, M.; Goddard, R.; Lehmann, C. W. *Angew. Chem., Int. Ed.* **2008**, *47*, 3210−3214.

(29) For a mechanistic proposal involving amine nucleophiles, see ref 12g.

(30) For examples, see: (a) Cheong, P. H.; Morganelli, P.; Luzung, M. R.; Houk, K. N.; Toste, F. D. *J. Am. Chem. Soc.* **2008**, *130*, 4517. (b) Kovács, G.; Ujaque, G.; Lledós, A. *J. Am. Chem. Soc.* **2008**, *130*, 853. (c) Bo, C.; Maseras, F. *Dalton Trans.* **2008**, 2911. (d) Paton, R. S.; Maseras, F. *Org. Lett.* **2009**, *11*, 2237. (e) Liu, L.-P.; Malhotra, D.; Paton, R. S.; Houk, K. N.; Hammond, G. B. *Angew. Chem., Int. Ed.* **2010**, *49*, 9132−9135.

(31) (a) Kozuch, S.; Shaik, S. *J. Phys. Chem. A* **2008**, *112*, 6032−6041. (b) Kozuch, S.; Shaik, S. *Acc. Chem. Res.* **2011**, *44*, 101−110.

(32) Brown, T. J.; Weber, D.; Gagné, M. R.; Widenhoefer, R. A. *J. Am. Chem. Soc.* **2012**, *134*, 9134−9137.